

# Chapter 1

## A Brief Review of III-Nitride UV Emitter Technologies and Their Applications

Michael Kneissl

**Abstract** This chapter provides a brief introduction to group III-nitride ultraviolet light emitting diode (LED) technologies and an overview of a number of key application areas for UV-LEDs. It covers the state of the art of UV-LEDs as well a survey of novel approaches for the development of high performance UV light emitters.

### 1.1 Background

More than two decades have passed since a series of fundamental breakthroughs in the area of gallium nitride (GaN) semiconductor materials led to the first demonstration of high efficiency and high brightness blue LEDs [1–4]. Today, GaN-based blue and white LEDs have achieved efficiencies surpassing that of any conventional light source and billions of LEDs are fabricated every week. This tremendous progress has been accompanied by increasing penetration of blue and white LEDs into new applications and larger markets, starting with backlighting of LCD displays in mobile phones, computer screens, and TVs, followed by automotive and street lighting, and finally conquering lighting applications in all places. Therefore, it is only fitting that in 2014 the Royal Swedish Academy of Sciences awarded the Nobel Prize for Physics to Isamu Akasaki, Hiroshi Amano, and Shuji Nakamura “for the invention of efficient blue light emitting diodes which has enabled bright and energy-saving white light sources” [5]. This example shows how breakthroughs in development of new semiconductor materials and device technologies can lead to a paradigm shift of a complete industry, in this case solid-state lighting. The Royal Swedish Academy of Sciences stated in their press release “in the spirit of Alfred

---

M. Kneissl (✉)

Institute of Solid State Physics, Technische Universität, Berlin, Germany  
e-mail: kneissl@physik.tu-berlin.de

M. Kneissl

Ferdinand-Braun-Institut, Leibniz-Institut für Höchstfrequenztechnik, Berlin, Germany

© Springer International Publishing Switzerland 2016

M. Kneissl and J. Rass (eds.), *III-Nitride Ultraviolet Emitters*,

Springer Series in Materials Science 227, DOI 10.1007/978-3-319-24100-5\_1

Nobel the Prize rewards an invention of greatest benefit to mankind; using blue LEDs, white light can be created in a new way” [5]. Despite these tremendous achievements, we have to date only utilized a very narrow sliver of the emission spectrum that gallium nitride devices are capable of generating. By adding aluminum nitride (AlN) to the GaN alloy system, the emission wavelength of AlGaIn-based LEDs can be tuned over almost the entire UVA (400–320 nm), UVB (320–280 nm), and UVC (280–200 nm) spectral range with emission wavelength as short as 210 nm. Although the efficiencies and power levels of AlGaIn-based UV-LEDs today are still modest (see Fig. 1.1) compared to their visible wavelength counterparts, another paradigm shift in the area of semiconductor-based UV sources is just around the corner. Without doubt the efficiencies and output powers of UV-LEDs will continue to improve over the coming years and at the same time the costs per milliwatt of UV light from LEDs will drop significantly. For many high-end applications, e.g., in the area of medical diagnostics, phototherapy, and sensing, UV-LEDs are already competitive since they enable major advances in system design and performance and only contribute a small fraction of the overall cost. As the UV-LED performance improves over time it is clear that many more application areas will follow.

In order to put all these developments into a context, this chapter will provide a comprehensive overview of the state of the art in group III-nitride-based materials,

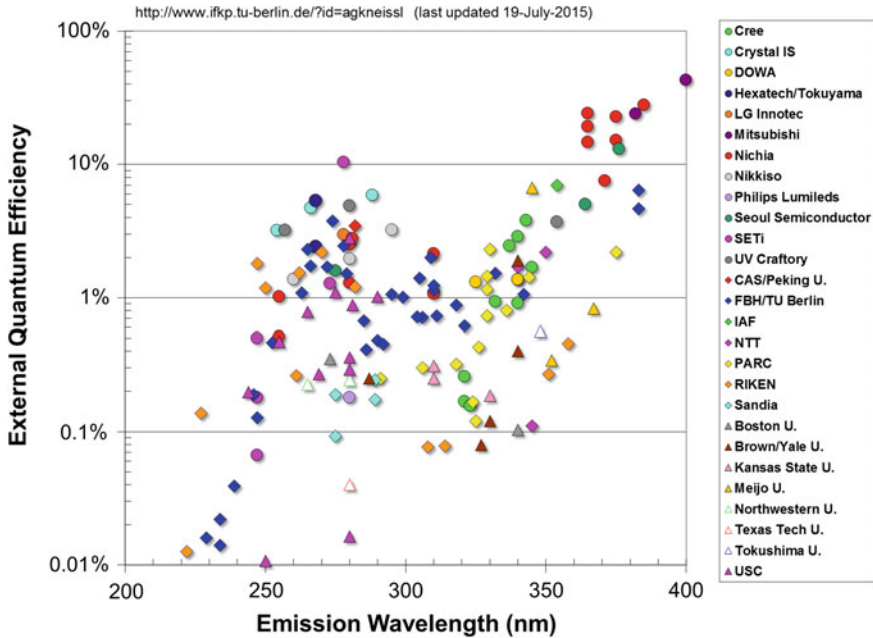


**Fig. 1.1** Reported external quantum efficiencies for AlGaIn, InAlGaIn-, and InGaIn quantum well LEDs emitting in the UV spectral range [6–32]

ultraviolet emitters, and their applications. Several key applications for UV emitters and detectors will be discussed, including water purification, phototherapy, gas sensing, fluorescence excitation, plant growth lighting, and UV curing. In addition, the optical, electronic, and structural properties of group III-nitride materials as well as the design and key performance parameters of UV-LEDs will be reviewed. Furthermore, the most important technological challenges for the realization of high efficiency, high power UV light emitters will be examined and a number of approaches to overcome these hurdles will be presented.

## 1.2 UV Light Emitters and Their Applications

Compared to conventional UV sources, such as low and medium pressure mercury lamps [33], ultraviolet LEDs offer a number of advantages. UV-LEDs are extremely robust, compact, environmentally friendly, and can exhibit very long lifetimes. They do not require any warm-up times and can be switched on and off within a few tens of nanoseconds or even faster. These unique properties designate UV-LEDs as a key enabling component for a number of new applications that cannot be realized with conventional UV sources. For example, the ability to rapidly turn UV-LEDs on and off gives rise to advanced measuring detection algorithms and improved baseline calibrations that can significantly enhance the sensitivity of the system. By closely spacing different UV-LEDs, it is also possible to realize multi-wavelength modules, which may be able to identify specific gases, biomolecules, or organisms. UV-LEDs are operated at moderate DC voltages, which make them ideally suited for battery operation or solar cell powering. They are also easily electronically dimmable, which can be an important energy saving feature, e.g., in water purification applications, where the required UV radiation dose strongly depends on the volume of the water flow. But most importantly, their emission can be tuned to cover any wavelength in the UVA (400–320 nm), UVB (320–280 nm), and UVC (280–200 nm) spectral range. A compilation of different applications for UV-LEDs is shown in Fig. 1.2. Important applications in the UVA spectral range include UV curing of inks, paints, coatings, resins, polymers, and adhesives as well as 3D-printing for rapid prototyping and lightweight construction. Additional applications can be found in the area of sensing, e.g., whitening agents or so-called blankophores, detection of security features, e.g., in ID cards and banknotes, and medical applications like blood gas analysis. Key applications in the UV-B are phototherapy [34, 35], especially the treatment of psoriasis and vitiligo, as well as plant growth lighting, e.g., for the targeted triggering of secondary plant metabolites [36]. High volume applications in the UVC are water purification [37–42], e.g., point-of-use systems, wastewater treatment, and recycling as well as disinfection of medical equipment and food. There are also a number of sensing applications [42–44] for UVB- and UVC-LEDs since many gases (e.g.,  $\text{SO}_2$ ,  $\text{NO}_x$ ,  $\text{NH}_3$ ) and biomolecules exhibit absorption bands in these spectral regions, including tryptophan, NADH, tyrosine, DNA, and RNA. UVC-LEDs can also be used for non-line-of-sight communication

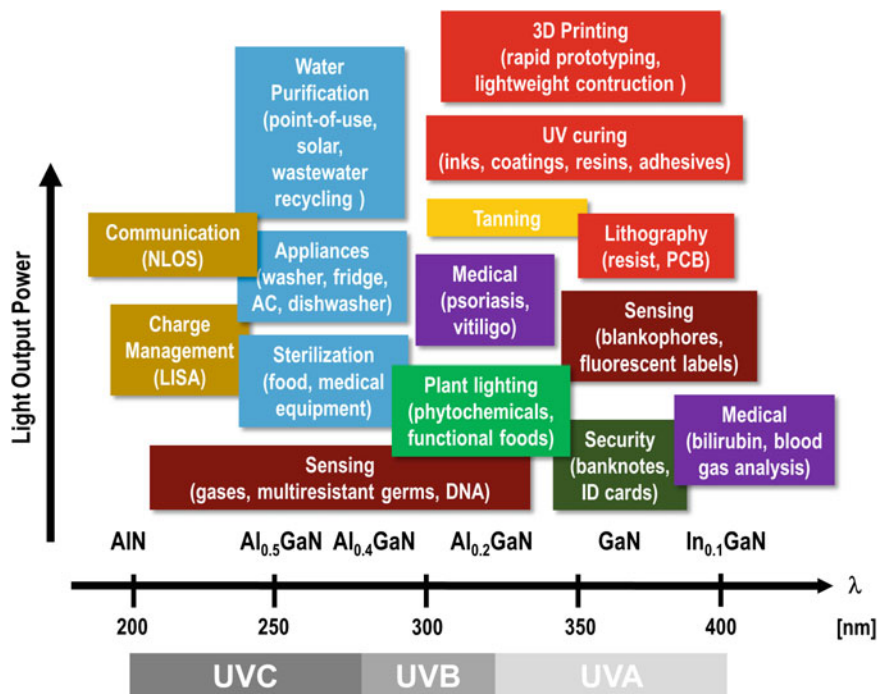


**Fig. 1.2** Applications of UVA (400–320 nm), UVB (320–280 nm), and UVC (280–200 nm) LEDs

[45] and are also of interest for basic science experiments in the area of gravitational sensors, e.g., for enabling the charge management systems in the ESA/NASA laser interferometer space antenna (LISA) mission [46]. The foundation of all these applications, however, is the development of high-efficiency and high power AlGaIn-based LEDs emitting in the UVA, UV-B, and UVC spectral range.

Thus, the economic and societal benefits resulting from the development of a wide range of applications that require UV-LED technologies are perfectly obvious. Latest market studies predict rapid technological advances in the development of semiconductor-based UV-LED sources. For the world market of UV-LED components alone an annual growth rate of more than 28 % is being forecasted by Yole Développement, reaching a total volume of US\$ 520 million by 2019 [47].

### 1.3 UV-LEDs—State of the Art and the Challenges Ahead

A large number of research groups have reported AlGaIn-based light emitting diodes in the ultraviolet spectral range [6–32] and several companies have started to commercialize UV-LED devices. In the 365–400 nm spectral range, many

companies are already offering UVA-LEDs with excellent performance. Companies include for example, Nichia (Japan), Nitride Semiconductors (Japan), Epitex (Japan), UVET Electronics (China), Tekcore (Taiwan), Seoul Opto Device (Korea), SemiLEDs (USA), Luminus Devices (USA), Lumex (USA), and LED Engine (USA). Access to commercial UVB-LEDs is much sparser with companies SETi (USA), Dowa (Japan), Nikkiso (Japan), and UVphotonics (Germany) offering devices in the 320–280 nm range. Similarly in the UVC, only a few companies are currently selling LED devices, including SETi (USA), Nitek (USA), Crystal-IS/Asahi-Kasei (USA/Japan), Hexatech (USA), UVphotonics (Germany), Nikkiso (Japan), and LG Electronics (Korea). Whereas the performance for UVA-LEDs, especially in the wavelength range 365–400 nm is already suitable for many applications, the external quantum efficiencies (EQE) of most UVB and UVC emitters are still in the single digit percentage range. Currently, most UVB- and UVC-LEDs provide only a couple of milliwatts of output power and lifetimes are often limited to less than a thousand hours [30, 41]. There are multiple reasons which limit the performance of group III-nitride-based deep UV-LEDs and nearly every layer in the heterostructure poses a different challenge as illustrated in Fig. 1.3.

Most UV-LED heterostructures are grown on (0001) oriented c-plane sapphire substrates. Sapphire substrate are readily available in various sizes with diameters ranging from 2 to 8-in. for commercial wafers and 12-in. diameter sapphire substrates already being demonstrated as R&D samples [49]. Due to the large volumes of sapphire substrates that are being used for blue LED production, sapphire wafers have become very inexpensive. Most importantly, sapphire is fully transparent across the entire UVA, UVB, and UVC spectral range due its large bandgap energy of 8.8 eV. Most AlGaIn-based LED heterostructures are grown by metalorganic

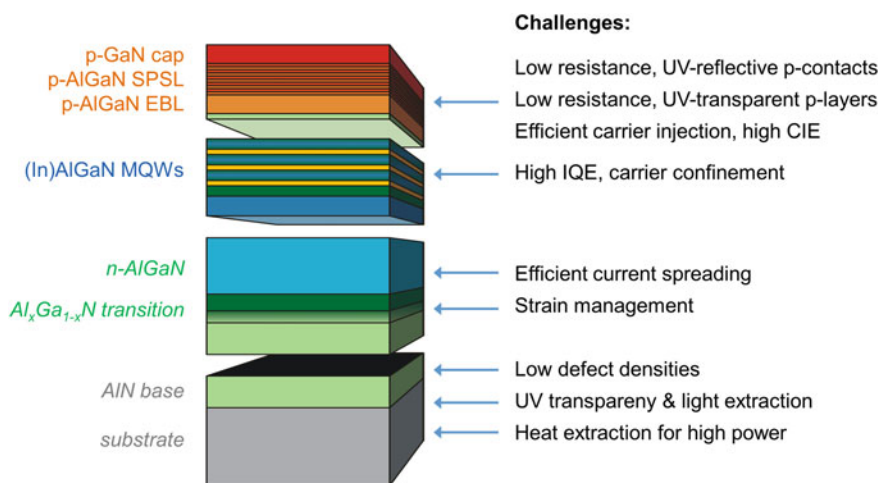


**Fig. 1.3** Schematic of an (In)AlGaIn MQW UV-LED heterostructure [48]

vapor phase epitaxy (MOVPE) using trimethylgallium (TMGa), triethylgallium (TEGa), trimethylaluminum (TMAI), and trimethylindium (TMIn) as group-III precursor, as well as ammonia (NH<sub>3</sub>) for the group-V element. Silane (SiH<sub>4</sub>) and di(cyclopentadienyl)magnesium (Cp<sub>2</sub>Mg) are used as n- and p-doping sources and hydrogen or nitrogen as carrier gas. Typical growth temperatures for the deposition of AlGa<sub>x</sub>N layers are in the range of 1000–1200 °C, but can be as high as 1500 °C for the deposition of the AlN base layer [50–52]. Since the sapphire substrate is electrically insulating an Si-doped n-AlGa<sub>x</sub>N current spreading layer is subsequently deposited to enable uniform lateral current-spreading and injection of electrons into the AlGa<sub>x</sub>N multiple quantum well (MQW) active region. In order to accommodate the difference in the a-lattice constants of AlGa<sub>x</sub>N and AlN (see Fig. 1.6), an Al<sub>x</sub>Ga<sub>1-x</sub>N transition layer is inserted between the AlN base and the AlGa<sub>x</sub>N current spreading layer for strain management. The light emitting active region typically comprises a few nanometer thick AlGa<sub>x</sub>N or InAlGa<sub>x</sub>N quantum wells (QWs) separated by (In)AlGa<sub>x</sub>N quantum barriers. The emission wavelength of the LEDs is primarily determined by the aluminum and indium mole fractions in the AlGa<sub>x</sub>N or InAlGa<sub>x</sub>N quantum wells as can be seen in Fig. 1.4a.

Additional contributions to the transition energies and consequently the emission wavelength arise from the electron and hole confinement energies in the quantum well and depend on the QW width as well as the quantum barrier height, i.e., the barrier composition. Figure 1.4b shows the emission wavelength of Al<sub>0.72</sub>Ga<sub>0.28</sub>N triple quantum well LEDs with Al<sub>0.82</sub>Ga<sub>0.18</sub>N barriers and different QW widths. Since almost all UV-LEDs are grown on the polar c-plane of the wurtzite crystal, strong spontaneous and piezoelectric polarization charges arise at AlGa<sub>x</sub>N heterostructure interfaces, leading to polarization fields in the QWs and consequently to a redshift in emission wavelength. This effect is commonly known as

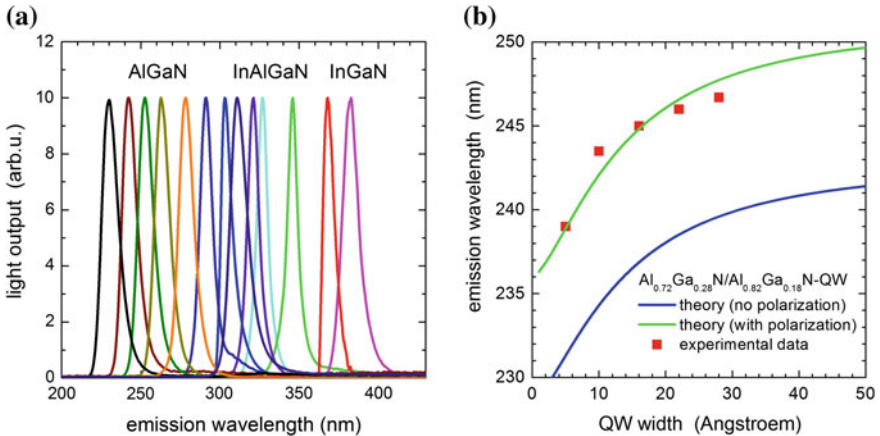


**Fig. 1.4** **a** Emission spectra of AlGa<sub>x</sub>N, InAlGa<sub>x</sub>N, and InGa<sub>x</sub>N quantum well LEDs emitting in the UVA, UVB, and UVC spectral range. **b** Emission wavelength of Al<sub>0.72</sub>Ga<sub>0.28</sub>N quantum well LEDs for different QW width

the quantum confined Stark effect (QCSE) [53]. The magnitude of the polarization field will largely depend on the difference in the aluminum mole fractions between the AlGaIn quantum wells and AlGaIn barriers as well as the strain state with the QW stack.

The active region is capped with an Mg-doped p-AlGaIn electron blocking layer (EBL), followed by an Mg-doped p-AlGaIn short period superlattice layer (SPSL) and a highly Mg-doped p-GaN ohmic contact layer. The function of the p-AlGaIn electron blocking layer (EBL) is to facilitate efficient hole injection into the QW active region while preventing electron leakage from the AlGaIn QW active region into the p-layers. Ideally, the Mg-doped p-AlGaIn SPSL is UV-transparent in order to prevent the absorption of UV photons. Looking at the different implementations of UV-LEDs in the literature, of course, there are many deviations from this basic UV-LED structure. For example, instead of a p-AlGaIn short period superlattice layer, an Mg-doped bulk p-AlGaIn layer can also be used. Some LED heterostructure designs utilize a gradient of the aluminum mole fraction in the p-AlGaIn layer in order to enhance the hole carrier concentrations through polarization doping [54]. Nevertheless, the key elements described above and in Fig. 1.3 can be found in most UV-LEDs. While metalorganic vapor phase epitaxy (MOVPE) is the dominant growth technique for the realization of UV-LEDs, AlGaIn-based UV light emitters have also been demonstrated using molecular beam epitaxy (MBE) [55] or hydride vapor phase epitaxy (HVPE) [56].

## 1.4 UV-LEDs—Key Parameters and Device Performance

There are several key parameters that characterize the performance characteristics of UV-LEDs. The conversion efficiency by which the electrical input power is converted into UV light output is described by the so-called wall plug efficiency (WPE) or power conversion efficiency (PCE). In general, the wall plug efficiency of light emitting diodes is defined as the ratio of the total UV output power to the input electrical power, i.e., the drive current times the operating voltage of the device. This can be described by the following relationships:

$$\text{WPE} = \frac{P_{\text{out}}}{I \cdot V} = \eta_{\text{EQE}} \frac{\hbar\omega}{e \cdot V},$$

where  $P_{\text{out}}$  denotes the output power of the UV emission,  $I$  the drive current of the LED,  $V$  the operating voltage for the LED,  $\hbar\omega$  the photon energy, and  $\eta_{\text{EQE}}$  the external quantum efficiency (EQE) of the LED. The external quantum efficiency of the UV-LED can be easily determined by measuring the total UV output power  $P_{\text{out}}$  and dividing this by the drive current  $I$  and the photon energy  $\hbar\omega$  according to the following equation:



$$\eta_{\text{EQE}} = \frac{e \cdot P_{\text{out}}}{I \cdot h\omega}$$

In other words, the EQE can also be described as the ratio of the number of UV photons emitted from the LED to the number of charge carriers injected into the device. The external quantum efficiency itself can be described as a product of the injection efficiency  $\eta_{\text{inj}}$ , the radiative recombination efficiency  $\eta_{\text{rad}}$ , and the light extraction efficiency  $\eta_{\text{ext}}$  as also shown in the following formula:

$$\eta_{\text{EQE}} = \eta_{\text{inj}} \cdot \eta_{\text{rad}} \cdot \eta_{\text{ext}} = \eta_{\text{IQE}} \cdot \eta_{\text{ext}}$$

Therefore, the injection efficiency  $\eta_{\text{inj}}$  describes the ratio of charge carriers, i.e., electrons and holes that reach the QW active region versus the total current being injected into the device. The radiative recombination efficiency  $\eta_{\text{rad}}$  is the fraction of all electron–hole pairs that recombine radiatively in the QW active region, i.e., producing UV photons. The internal quantum efficiency  $\eta_{\text{IQE}}$  (or IQE) can be calculated as the product of the radiative recombination efficiency  $\eta_{\text{rad}}$  and the injection efficiency  $\eta_{\text{inj}}$ . It is possible to determine the IQE by temperature and excitation power-dependent photoluminescence measurements [57], although great care has to be taken in the interpretation of the data. The light extraction efficiency  $\eta_{\text{ext}}$  is defined as the fraction of UV photons that can be extracted from the LED compared to all the UV photons that are generated in the active region. The radiative recombination efficiency  $\eta_{\text{rad}}$  can be expressed as the ratio of the radiative recombination rate  $R_{\text{sp}}$  versus the sum of radiative and nonradiative recombination  $R_{\text{nr}}$  rates and is described by the following equation:

$$\eta_{\text{rad}} = \frac{R_{\text{sp}}}{R_{\text{sp}} + R_{\text{nr}}}$$

The nonradiative recombination rate can be expressed as the sum of the Shockley–Read–Hall recombination term and the Auger recombination term as follows:

$$R_{\text{nr}} = A \cdot n + C \cdot n^3,$$

where  $A$  represents the Shockley–Read–Hall (SRH) recombination coefficient,  $C$  the Auger recombination coefficient, and the parameter  $n$  the charge carrier density in QW. The Shockley–Read–Hall recombination coefficient  $A$  is inverse proportional to the SRH recombination lifetime, which strongly depends on the defect density in the materials. Nonradiative recombination lifetimes as short as a few tens of ps have been measured for highly defective AlGaN layers. In contrast, nonradiative recombination lifetimes in the ns range have been demonstrated for AlGaN quantum well emitters on low defect density bulk AlN substrates [58, 59]. The magnitude of the Auger recombination coefficient  $C$  for III-nitride materials is still being heavily debated [60–65] and values for the  $C$  coefficient for blue-violet



LEDs range between  $1 \times 10^{-31}$  and  $2 \times 10^{-30} \text{ cm}^6 \text{ s}^{-1}$ . Measurements to determine the  $C$  coefficient for UV emitter are even more rudimentary [66]; also theoretical models suggest that the Auger coefficient should become smaller and smaller for shorter emission wavelength [67].

Finally, the radiative recombination or spontaneous recombination rate  $R_{\text{sp}}$  can be expressed as

$$R_{\text{sp}} = B \cdot n^2,$$

with  $B$  representing the bimolecular recombination coefficient and  $n$  the charge carrier density in QW. The  $B$  coefficient will strongly depend on the design of the active region, e.g., the quantum well width, quantum barrier height, the strain state of the AlGaIn QWs, and the magnitude of the polarization field in the QW. Typical values for the  $B$  coefficient are in the range of  $2 \times 10^{-11} \text{ cm}^3 \text{ s}^{-1}$  [66, 68].

Today, the best InGaIn-based blue LEDs boast external quantum efficiencies (EQE) of 84 % and wall plug efficiencies (WPE) of 81 % [69] and commercial blue LEDs exhibit EQEs of 69 % and WPEs of 55 %, respectively [70]. These extraordinary values can only be achieved by perfecting all constituents that contribute to the WPE and EQE. Due the development of thin film LED technologies, highly reflective metal contacts, and advanced packaging methods, light extraction efficiencies in modern blue LEDs exceed 85 %. Furthermore, low defect density GaN/sapphire templates and highly efficient InGaIn quantum well active regions lead to internal quantum efficiencies near 90 % [70]. Mg-doped GaIn AlGaIn electron blocking layers and low resistance  $n$ -GaN current spreading layers lead to injection efficiencies well beyond 90 % [70]. And finally, refined Mg- and Si-doping profiles and optimized ohmic contacts guarantee very low operating voltages, which translate into high WPE. However, the extraordinary characteristics of blue LEDs do not translate into similar performance for shorter wavelength LEDs. Whereas UVA-LEDs near 365 nm still exhibit EQEs beyond 30 %, at least in research prototypes, typical LEDs in the UV-B and UVC spectral range exhibit external quantum efficiencies of 1–3 %, as can be seen in Fig. 1.1. A number of factors contribute to this overall small value, including poor radiative recombination efficiencies and modest injection efficiencies, resulting in low internal quantum efficiencies as well as inferior light extraction and high operating voltages. From the analysis of state-of-the-art UVC-LED one can estimate the light extraction efficiency to be below 10 %, and the radiative and injection efficiencies to be somewhere around 50 %, respectively. In the following section the main causes contributing to these behaviors will be explained and different options to overcome these deficiencies will be discussed.

## 1.5 The Role of Defects on the IQE of UV-LEDs

A significant contribution to the low IQE in UV emitters can be attributed to the relatively high defect densities in AlN and AlGaIn materials. For example, growth of AlN layers on (0001) sapphire substrates typically yields dislocation densities in the range of  $10^{10} \text{ cm}^{-2}$  [50–52]. These threading dislocations form nonradiative recombination pathways for the injected carriers leading to significantly reduced internal (IQE) and external quantum efficiencies (EQE) [57, 70, 71]. Different approaches to reduce the dislocation densities in AlGaIn and AlN layers on sapphire substrates have been demonstrated, including epitaxial lateral overgrowth (ELO) yielding defect densities in the mid  $10^8 \text{ cm}^{-2}$  range [72–76]. Other approaches to reduce the defect density include the growth on nano-patterned sapphire substrates [29, 77], the use of short period AlGaIn superlattices [78] as well as low temperature AlN or SiN<sub>x</sub> interlayers [18, 79]. To estimate the effect of dislocations on the internal quantum efficiency of UV-LEDs the IQE was simulated based on a model initially published by Karpov et al. [71]. In order to compute the IQE, the radiative and nonradiative recombination rates are calculated as a function of the threading dislocation density and injection current density [23]. The model assumes that threading dislocations form deep levels within the band gap that act as nonradiative recombination centers for electrons and holes. There are a number of potential defects in AlGaIn wurtzite semiconductor materials that form deep levels, e.g., screw, edge, or mixed type threading dislocations as well as N- or Ga-vacancies [80–83]. Although the nature of the dislocation and its electronic properties is not part of the model, the parameter  $S$  in the simulation characterizes the fraction of electrically active sites on the dislocation core. In addition, the IQE is governed by the electron and hole mobilities, nonequilibrium carrier concentrations, and consequently the minority carrier diffusion lengths. As can be seen from the results of the simulation in Fig. 1.5a, dislocation densities in the range of  $10^7 \text{ cm}^{-2}$  are required in order to provide internal quantum efficiencies close to unity. By utilizing advanced dislocation filtering techniques, one could expect to realize dislocation densities in this range even for heteroepitaxial growth on sapphire substrates. As can also be seen from Fig. 1.5b, for a fixed threading dislocation density, the IQE also strongly depends on the electron mobility and current density. This dependency is most pronounced for dislocation densities ranging between mid  $10^8$  and  $10^{10} \text{ cm}^{-2}$ , when the carrier diffusion lengths and the spacing of the dislocations are approximately the same size (Fig. 1.6).

Even lower defect densities can be achieved by homoepitaxial growth on bulk AlN substrates. For example, bulk AlN substrates grown by sublimation recondensation have yielded dislocation densities as low as  $10^4 \text{ cm}^{-2}$  [84–87], although the availability of these substrates is still limited and currently typical substrates sizes are 1-in. diameter or even smaller. In addition bulk AlN substrates exhibit strong absorption bands in the UVC spectral range [88, 89], which poses a serious challenge for the light extraction, since this is normally achieved by extracting the UV light through the substrate. As various studies show, the origin of these UVC

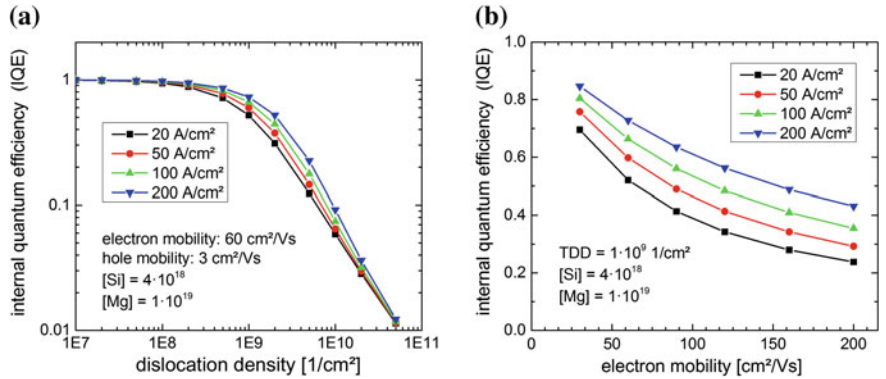
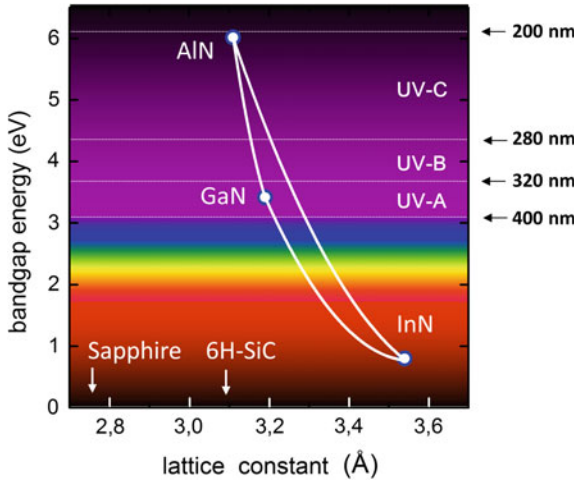


**Fig. 1.5** Simulated internal quantum efficiencies (IQE) for an AlGaN MQW LED emitting near 265 nm. **a** IQE versus threading dislocation density in the active region for different current densities. **b** IQE versus the electron mobility for different current densities (simulations are courtesy of Martin Guttman and Christoph Reich, Institute of Solid State Physics, TU Berlin)

absorption bands can be traced back to carbon impurities and the formation of complexes [88–90]. Therefore these UVC absorption bands appear to be not a fundamental problem, but a materials research challenge that can be solved by optimizing the purity of the sources in order to reduce the carbon impurity concentrations either by clever co-doping schemes, or by inserting a thick hydride vapor epitaxy grown AlN base layer [91]. UVC-LED heterostructures pseudomorphically grown on bulk AlN substrate have been demonstrated by two groups [22, 92] with external quantum efficiencies of more than 5 % at emission wavelength near 270 nm and first steps to commercialize these devices have been undertaken.

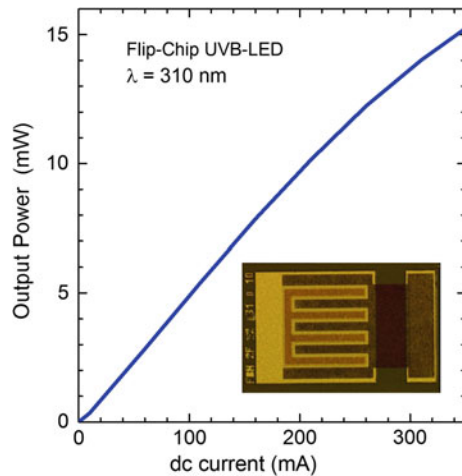
**Fig. 1.6** Bandgap energies and emission wavelength of InN, GaN, AlN and other III–V and II–VI compound semiconductor materials plotted versus their lattice spacing



## 1.6 Current-Injection Efficiency and Operating Voltages of UV-LEDs

Very often UV-LEDs suffer from poor injection efficiencies and high operation voltages that originate from the relatively low conductivities of Mg-doped p-AlGaN layers. This is due to the fact that the ionisation energy for the Mg acceptor increases steadily with the aluminum mole fraction in the Mg-doped p-AlGaN layer [93, 94]. For Mg-doped AlN layers the acceptor level has been determined to be about 510 meV above the valence band edge [70]. Therefore, in Mg-doped bulk AlGaN layers only a small fraction of the Mg acceptors are ionized at room temperature, resulting in very low free hole concentrations. But even the silicon doping on n-AlGaN layers becomes increasingly more challenging at high aluminum mole fractions [95–97]. Both n- and p-AlGaN layer resistances as well as the ohmic contact resistances of the n- and p-metals contribute to the relatively high operating voltages of UV light emitting devices. Various approaches to improve the conductivity of p-AlGaN layers have been explored, e.g., utilizing short period  $\text{Al}_x\text{Ga}_{1-x}\text{N}/\text{Al}_y\text{Ga}_{1-y}\text{N}$  superlattices [98, 99], polarization doping of graded  $\text{Al}_x\text{Ga}_{1-x}\text{N}$  layers [100], and alternative p-layer materials like Mg-doped boron nitride (hBN) [101]. Also, the limits of silicon doping of n-AlGaN layers at very high aluminum mole fractions have been explored and record low resistivity AlGaN: Si current-spreading layers in the composition range between 60 and 96 % have been demonstrated [102, 103]. A number of studies have looked at ohmic metal contact formation to n-AlGaN layers and lowering the contact resistances [104–108] with very promising results in the medium aluminum composition range. Since sapphire and AlN substrates are electrically insulating, electrons are normally laterally injected through the n-AlGaN layer. In order to reduce the n-layer series resistance and to facilitate homogeneous current injection often interdigitated finger contact geometries are employed in the chip design. Figure 1.7 shows a photograph of an

**Fig. 1.7** Light-output versus current ( $L-I$ ) characteristic of a flip-chip mounted UVB-LED on a ceramic package. The *inset* shows a photograph of the LED chip with interdigitated finger contacts before mounting



UVB-LED chip with interdigitated finger contacts and its light-output versus current ( $L$ – $I$ ) characteristic after flip-chip mounting.

Another key challenge is efficient hole injection into the AlGaIn quantum wells as well as electron leakage from the active region. Injection efficiency and electron leakage are two properties that are difficult to determine in a UV-LED and can range from less than 10 % for deep UV emitters to more than 90 % for UVA-LEDs near 400 nm [70, 109]. Especially for UVB- and UVC-LEDs, the development of novel injection schemes is critical in order to reduce electron leakage while improving hole-injection efficiencies into the active region. On this topic, various approaches have been demonstrated, e.g., Mg-doped AlGaIn electron blocking layers, AlN/AlGaIn electron blocking heterostructures [28, 31], and AlGaIn/AlGaIn multi-quantum-barriers [19].

### 1.7 Light Extraction from UV-LEDs

Improving light extraction from UV-LEDs is a key challenge in order to increase the EQE and WPE of UV-LEDs. Currently, most UV-LED chips do not include any features for advanced light extraction. As can be seen from Table 1.1, the light extraction efficiency for a single square LED chip on a UV-transparent sapphire substrate is only in the range of 8–10 % [110]. This is due to the fact that many of the light extraction methods that are state of the art for blue and near UV-LED cannot be applied to deep UV-LEDs. For example, highly reflective and low resistance silver-based metal contacts are typically employed in blue LEDs. Although Ag contacts provide excellent reflectors in the visible and near UV range, the reflectivity drops rapidly for wavelength below 350 nm (see e.g., Chap. 6). Aluminum, which would be a very good reflector in the entire UV range and possible alternative contact material does not normally form an ohmic contact to Mg-doped p-AlGaIn due to its low work function. In addition, thin film technologies that are routinely applied to GaN-based LEDs have not yet been developed

**Table 1.1** Estimated light extraction efficiencies (LEE) for different UV-LEDs chip technologies

UV-LED chip technology	LEE (%)
LED on-wafer	7–9
Single square LED chip	8–10
Single triangular LED chip	11–13
LED with reflective p-contact ( $R = 40$ %)	~ 20
LED with reflective p-contact ( $R = 80$ %)	~ 30
Thin film LED chip, incl. backside roughening	30–50
Thin film LED chip with reflective contacts and backside roughening	40–60
Thin film LED with reflective contacts and backside roughening and advanced packaging	50–90

for deep UV emitters. Ultraviolet light also poses an enormous challenge in finding suitable encapsulation and packaging materials. Many advanced packaging materials, i.e., high-index transparent silicones and polymers, that are state of the art for blue LEDs, are not stable when exposed to high energy UV photons. Therefore completely new solutions have to be developed for AlGaIn-based deep UV emitters and several approaches to enhance light extraction have been investigated including photonic crystals, roughening of LED surfaces, patterning of substrates, shaping of LED dies, micro-pixel LEDs, and omnidirectional reflectors [111–115]. Another approach to realize ohmic and UV-reflective contacts are nano-pixel LEDs. In this case low resistance ohmic contacts are facilitated through closely spaced nano-pixel size Pd/p-GaN electrodes while the area between the nano-pixels is covered with UV-reflective aluminum reflectors [116].

An additional complication arises from the large negative crystal field splitting in AlGaIn alloys. This causes a rearrangement of the valence bands at higher aluminum mole fraction resulting in a change in the polarization of light emission from TE to TM at shorter wavelength [117]. Consequently, fewer photons can be extracted from the light escape cone via the surface or the substrate of deep UV-LEDs. Although the basic properties of AlN materials cannot be changed, the optical polarization of the light emission can be controlled by the design of the AlGaIn quantum well active region and the built-in compressive or tensile strain. Recent studies have shown that even at very short wavelengths below 250 nm the polarization of emission from LEDs can be switched to strongly TE-polarized emission by employing highly compressively strained AlGaIn active regions [118–121] and by appropriately adjusting the quantum well width and barrier height [122]. In addition, by employing reflector and scattering structures in advanced UVC-LED chip designs, enhanced outcoupling of TM polarized emission was recently demonstrated [123, 124].

## 1.8 Thermal Management and Degradation of UV-LED

Since the UV-LED light output as well as LED degradation is highly temperature-dependent, thermal management is pivotal for high performance UV light emitters [125, 126, 127]. Many LED failure mechanisms can also be traced back to overheating. Therefore most high-power UV-LEDs are flip-chip mounted onto ceramic submounts or directly integrated into SMD (surface-mount device) packages. Flip-chip mounting allows for efficient light extraction through the UV-transparent sapphire substrate and at the same time provides excellent heat extraction for thermal management. Typical packaging materials, e.g., include AlN and BN ceramics as well as aluminum, CuW, and copper. In order to dissipate the power generated at the contacts and pn-junction of the LED, the excess heat must be extracted through the package. Since only a small fraction of the excess power can be dissipated by radiation or convection from the LED chip, the heat extraction is mostly conducted through the package. The thermal resistance of the package is

hereby given by the sum of the thermal resistance of the LED die, the die attach, the heatsink, and finally the solder attaching the package to the board. Of course for the total thermal resistance the thermal resistances of the solder pads and the mounting board (e.g., PCB) also have to be added. Package thermal resistance can vary greatly depending on the packaging technologies. Top-emitting low power UV-LEDs, where the heat is extracted through the sapphire substrate can exhibit thermal resistance in the range of 40 K/W to more than 200 K/W depending on the packaging technology [128]. On the other hand flip-chip mounted UV-LEDs in high power packages can yield thermal resistances from 15 K/W to less than 5 K/W [129].

Another complex issue is the degradation of UV-LEDs. Early devices exhibited rapid degradation and very short lifetimes, especially for UVB- and UVC-LEDs [39, 41]. In some cases the output power dropped by more than 50 % within the first 100 h of operation, rendering these LEDs impractical for real-world applications. Next to increasing the LED efficiencies, improving the lifetimes of UV-LEDs is one of the key issues to solve in order to enable a broader integration of UV-LEDs in many applications. Fortunately due to improvements in material quality, chip technology, and thermal management, significant improvements in UV-LED lifetimes can be observed as can be seen in Fig. 1.8. Today, state-of-the-art UVB-LEDs on sapphire emitting at 310 nm and near 280 nm exhibit L50 lifetimes of more than 10.000 h [130, 131] and 3.000 h [30]. For UVC-LEDs on bulk AlN substrates with emission below 270 nm L50 lifetimes well in excess of 1.000 h have been reported [132]. It is difficult to predict how fast progress in this area will be but a better understanding of the degradation mechanism of UV-LEDs will be pivotal in solving the lifetime issues [133, 134]. This, of course, is not only limited to the LED chip and the semiconductor materials, but also includes packaging and encapsulation materials.

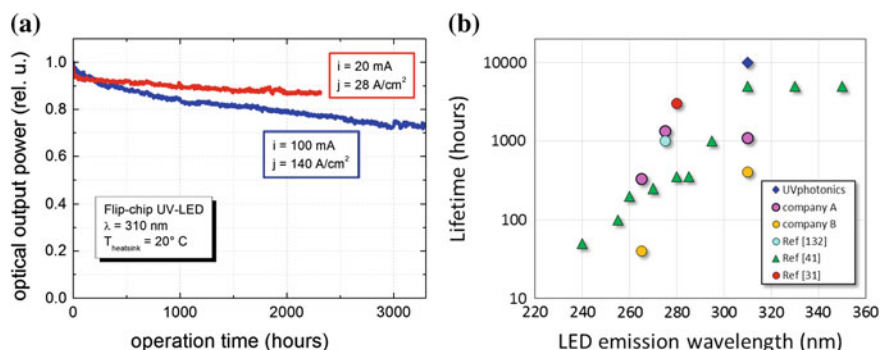


**Fig. 1.8** **a** Normalized change in UVB-LED output power over time. L<sub>50</sub> lifetimes of more than 10.000 h are expected. **b** Reported and measured lifetimes for UV-LEDs from different generations and emission wavelength



## 1.9 Outlook

Generally, it is a difficult undertaking to provide an accurate prognosis of the future performance of UV-LEDs. Nevertheless, by taking into account the rate of progress in the past decade as well as the potential improvements by implementing the different technological advances outlined in the earlier paragraphs, one can compile a roadmap for the future device performance. Based on these assumptions Fig. 1.9a, b displays the projected device performance for three wavelength bands around 310, 285, and 265 nm. Specifically, the past and future wall plug efficiencies and output power levels for single LEDs chips are plotted. The solid data points hereby represent the state of the art of commercially available UV-LED devices at different times up to 2015. It should be noted that these values have been obtained by measurements in our laboratory. In addition, the number of tested devices was limited due to the scant number of commercial sources for UVB- and UVC-LEDs and that devices were not readily available from all commercial sources. There are a number of factors that will lead to future improvement of the wall plug efficiency (WPE), including increases in internal quantum efficiency, reduced operating voltages, and enhancements in light extraction. As the WPE is improving, the output power per UV-LED chip will also increase. In addition to efficiency improvements larger chip areas, improved thermal management, and increases in the operating current will lead to further increases in the total output power per LED chip. For example, today most UVB- and UVC-LEDs are operated at 20 or 100 mA DC current and the footprint of the emitting area is typically limited to less than  $0.1 \text{ mm}^2$ . It is expected that the chip size of UV-LEDs will increase to  $1 \text{ mm}^2$  and more, and operating currents of 350, 700 mA or even 1 A will become standard. The pace at which these improvements are implemented, will of course also depend on the amount of effort that goes into the research and development for these

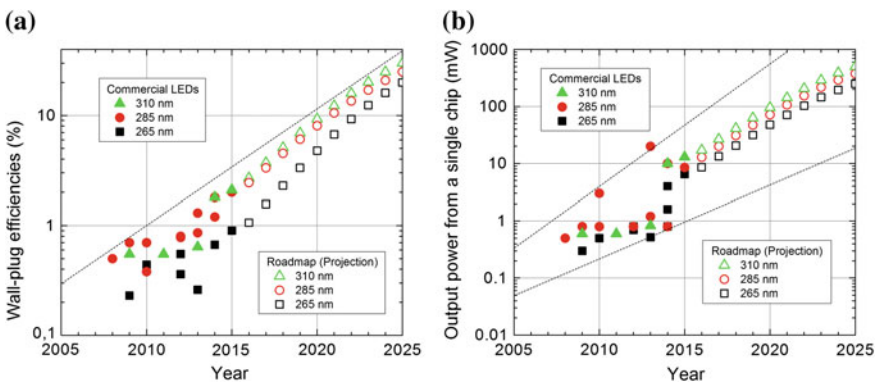


**Fig. 1.9** Actual and projected wall plug efficiencies **a** as well as light output power **b** of production scale UV-LEDs in the wavelength band around 310, 285, and 265 nm. The *dotted lines* provide the upper and lower limits for the prognosis and are also an indicator for the uncertainty in the projection

devices. Fortunately, it appears that research efforts in the development of UV light emitters have significantly accelerated in the past few years and that more and more larger industry players (e.g., Nichia, LG Innotek, Panasonic) are getting involved.

## 1.10 Summary

Since the first demonstration of UV light emitting diodes in the early 1990s [135] and first AlGaIn-based LEDs in early 2000 [136–138], steady progress has been made in the development of ultraviolet LEDs. For a number of reasons however, the rate of progress in UV emitter performances was much slower than for GaN-based blue and white LEDs. The various technological challenges have been discussed in this chapter. One additional reason is the enormous variety of applications for UV emitters. This makes UV-LEDs on the one hand extremely versatile, but on the other hand it hinders the rapid development of UV devices due to the strongly varying requirements (i.e., emission wavelength, power levels, lifetimes) depending on the application. Overall, the development of group III-nitride UV emitters can be divided into three stages. The first phase was characterized by fundamental materials breakthrough and basic proof of device operation. This stage was followed by steady progress in device technologies and UVB- and UVC-LED performance as well as maturing of UVA-LEDs and their widespread adoption in applications like UV curing. We have now entered the third phase, which is characterized by an increasing number of companies and especially larger players entering the commercial markets. This will accelerate the development pace of UVB- and UVC-LEDs and soon the performance level will reach the threshold to enable first applications in the area of sensing, medical diagnostics, phototherapy, and point-of-use water disinfection. It is not an overstatement to say that there are no fundamental technological roadblocks prohibiting the realization of long-lived, high power and high efficiency UV-LED in the entire UV spectral range. Without exaggeration one can state that AlGaIn-based LEDs will prevail as UV emitter technology and that in the not too distant future we will see more and more applications that are enabled by UV-LEDs.

**Acknowledgment** This review would not have been possible without the commitment of numerous Ph.D. students, postdoctoral researchers, colleagues, and collaborators over many years resulting in a large number of joint publications, many of which are also referenced in this book chapter. Without emphasizing anyone in particular I would like to thank all of these individuals for their contributions. I also like to acknowledge the financial support by a number of funding agencies, starting with the DARPA “SUVOS” program that ran in the United States between 2002 and 2006. Since my return to Germany I gratefully acknowledge support by the German Research Foundation (DFG) within the Collaborative Research Center “Semiconductor Nanophotonics” (CRC 787) as well as funding by the Federal Ministry of Education and Research (BMBF) of Germany within the “Deep UV-LED” and “UltraSens” projects, the regional growth core “WideBaSe”, and the consortium “Advanced UV for Life” within the “Twenty20 – Partnership for Innovation” initiative. Finally, I would like to take this opportunity to thank my family, in particular my wife Rebecca, for her encouragement, continued support, and patience.

## References

1. I. Akasaki, H. Amano, K. Hiramatsu, N. Sawaki, High efficiency blue LED utilizing GaN film with AlN buffer layer grown by MOVPE. in *Proceedings of 14th International Symposium on Gallium Arsenide and Related Compounds 1987*, pp. 633–636 (1988)
2. S. Nakamura, T. Mukai, M. Senoh, High-power GaN p-n junction blue-light-emitting diodes. *Jpn. J. Appl. Phys.* **30**, L1998–L2001 (1991)
3. S. Nakamura, M. Senoh, T. Mukai, p-GaN/n-InGaN/n-GaN double-heterostructure blue-light-emitting diodes. *Jpn. J. Appl. Phys.* **32**, L8–L11 (1993)
4. S. Nakamura, T. Mukai, M. Senoh, Candeera-class high-brightness InGaN/AlGaIn double-heterostructure blue-light-emitting diodes. *Appl. Phys. Lett.* **64**, 1687–1689 (1994)
5. Press release of the The Royal Swedish Academy of Sciences. Retrieved 7 Oct 2014, [www.nobelprize.org/nobel\\_prizes/physics/laureates/2014/press.html](http://www.nobelprize.org/nobel_prizes/physics/laureates/2014/press.html).
6. “UV LED Efficiency 2015 (last update 19-July-2015)”. Retrieved 6 Oct 2015, [www.researchgate.net/publication/280131929](http://www.researchgate.net/publication/280131929)
7. T. Nishida, N. Kobayashi, T. Ban, GaN-free transparent ultraviolet light-emitting diodes. *Appl. Phys. Lett.* **82**, 1 (2003)
8. J. Edmond, A. Abare, N. Bergman, J. Bharathan, K.L. Bunker, D. Emerson, K. Haberern, J. Ibbetson, M. Leung, P. Russel, D. Slater, High efficiency GaN-based LEDs and lasers on SiC. *J. Cryst. Growth* **272**, 242 (2004)
9. M. Kneissl, Z. Yang, M. Teepe, C. Knollenberg, N.M. Johnson, A. Usikov, V. Dmitriev, Ultraviolet InAlGaIn light emitting diodes grown on hydride vapor phase epitaxy AlGaIn/sapphire template. *Jpn. J. Appl. Phys.* **45**, 3905 (2006)
10. Y. Taniyasu, M. Kasu, T. Makimoto, An aluminium nitride light-emitting diode with a wave-length of 210 nanometres. *Nature* **441**, 325 (2006)
11. H. Tsuzuki, F. Mori, K. Takeda, T. Ichikawa, M. Iwaya, S. Kamiyama, H. Amano, I. Akasaki, H. Yoshida, M. Kuwabara, Y. Yamashita, H. Kan, High-performance UV emitter grown on high-crystalline quality AlGaIn underlying layer. *Phys. Status Solidi (a)* **206**, 1199 (2009)
12. J.P. Zhang, A. Chitnis, V. Adivarahan, S. Wu, V. Mandavilli, R. Pachipulusu, M. Shatalov, G. Simin, J.W. Yang, M.A. Kahn, Milliwatt power deep ultra-violet light-emitting diodes over sapphire with emission at 278 nm. *Appl. Phys. Lett.* **81**, 4910 (2002)
13. V. Adivarahan, S. Wu, J.P. Zhang, R.A. Chitnis, M. Shatalov, V. Mandavilli, R. Gaska, M. A. Khan, High-efficiency 269 nm emission deep ultraviolet light-emitting diodes. *Appl. Phys. Lett.* **84**, 4762 (2004)
14. J. Zhang, X. Hu, A. Lunev, J. Deng, Y. Bilenko, T.M. Katona, M.S. Shur, R. Gaska, M.A. Khan, AlGaIn deep-ultraviolet light-emitting diodes. *Jpn. J. Appl. Phys.* **44**, 7250 (2005)
15. H. Hirayama, T. Yatabe, N. Noguchi, T. Ohashi, N. Kamata, 231–261 nm AlGaIn deep-ultraviolet light-emitting diodes fabricated on AlN multilayer buffers grown by ammonia pulse-flow method on sapphire. *Appl. Phys. Lett.* **91**, 071901 (2007)
16. A. Khan, K. Balakrishnan, T. Katona, Ultraviolet light-emitting diodes based on group three nitrides. *Nat. Photonics* **2**, 77 (2008)
17. S. Sumiya, Y. Zhu, J. Zhang, K. Kosaka, M. Miyoshi, T. Shibata, M. Tanaka, T. Egawa, AlGaIn-based deep ultraviolet light-emitting diodes, grown on epitaxial AlN/sapphire templates. *Jpn. J. Appl. Phys.* **47**, 43 (2008)
18. H. Hirayama, S. Fujikawa, N. Noguchi, J. Norimatsu, T. Takano, K. Tsubaki, N. Kamata, 222–282 nm AlGaIn and InAlGaIn-based deep-UV LEDs fabricated on high-quality AlN on sapphire. *Phys. Stat. Sol. (a)* **206**, 1176 (2009)
19. H. Hirayama, Y. Tsukada, T. Maeda, N. Kamata, Marked enhancement in the efficiency of deep-ultraviolet AlGaIn light-emitting diodes by using a multiquantum-barrier electron blocking layer. *Appl. Phys. Express* **3**, 031002 (2010)

20. A. Fujioka, T. Misaki, T. Murayama, Y. Narukawa, T. Mukai, Improvement in output power of 280-nm deep ultraviolet light-emitting diode by using AlGaIn multi quantum wells. *Appl. Phys. Express* **3**, 041001 (2010)
21. C. Pernot, M. Kim, S. Fukahori, T. Inazu, T. Fujita, Y. Nagasawa, A. Hirano, M. Ippommatsu, M. Iwaya, S. Kamiyama, I. Akasaki, H. Amano, Improved efficiency of 255–280 nm AlGaIn-based light-emitting diodes. *Appl. Phys. Express* **3**, 061004 (2010)
22. J.R. Grandusky, S.R. Gibb, M.C. Mendrick, C. Moe, M. Wraback, L.J. Schowalter, High output power from 260 nm pseudomorphic ultraviolet light-emitting diodes with improved thermal performance. *Appl. Phys. Express* **4**, 082101 (2011)
23. M. Kneissl, T. Kolbe, C. Chua, V. Kueller, N. Lobo, J. Stellmach, A. Knauer, H. Rodriguez, S. Einfeldt, Z. Yang, N.M. Johnson, M. Weyers, Advances in group III-nitride based deep UV light emitting diode technology. *Semicond. Sci. Technol.* **26**, 014036 (2011)
24. M. Shatalov, W. Sun, A. Lunev, X. Hu, A. Dobrinsky, Y. Bilenko, J. Yang, AlGaIn Deep-ultraviolet light-emitting diodes with external quantum efficiency above 10 %. *Appl. Phys. Express* **5**, 082101 (2012)
25. V. Kueller, A. Knauer, C. Reich, A. Mogilatenko, M. Weyers, J. Stellmach, T. Wernicke, M. Kneissl, Z. Yang, C.L. Chua, N.M. Johnson, Modulated epitaxial lateral overgrowth of AlN for efficient UV LEDs. *IEEE Photonics Tech. Lett.* **24**, 1603 (2012)
26. T. Kinoshita, T. Obata, T. Nagashima, H. Yanagi, B. Moody, S. Mita, S. Inoue, Y. Kumagai, A. Koukitu, Z. Sitar, Performance and reliability of deep-ultraviolet light-emitting diodes fabricated on AlN substrates prepared by hydride vapor phase epitaxy. *Appl. Phys. Express* **6**, 092103 (2013)
27. J.R. Grandusky, J. Chen, S.R. Gibb, M.C. Mendrick, C.G. Moe, L. Rodak, G.A. Garrett, M. Wraback, L.J. Schowalter, 270 nm pseudomorphic ultraviolet light-emitting diodes with over 60 mW continuous wave output power. *Appl. Phys. Express* **6**, 032101 (2013)
28. T. Kolbe, F. Mehnke, M. Guttman, C. Kuhn, J. Rass, T. Wernicke, M. Kneissl, Improved injection efficiency in 290 nm light emitting diodes with Al(Ga)N electron blocking heterostructure. *Appl. Phys. Lett.* **103**, 031109 (2013)
29. P. Dong, J. Yan, J. Wang, Y. Zhang, C. Geng, T. Wei, P. Cong, Y. Zhang, J. Zeng, Y. Tian, L. Sun, Q. Yan, J. Li, S. Fan, Z. Qin, 282-nm AlGaIn-based deep ultraviolet light-emitting diodes with improved performance on nano-patterned sapphire substrates. *Appl. Phys. Lett.* **102**, 241113 (2013)
30. A. Fujioka, K. Asada, H. Yamada, T. Ohtsuka, T. Ogawa, T. Kosugi, D. Kishikawa, T. Mukai, High-output-power 255/280/310 nm deep ultraviolet light-emitting diodes and their lifetime characteristics. *Semicond. Sci. Technol.* **29**, 084005 (2014)
31. F. Mehnke, C. Kuhn, M. Guttman, C. Reich, T. Kolbe, V. Kueller, A. Knauer, T. Wernicke, J. Rass, M. Weyers, M. Kneissl, Efficient charge carrier injection into sub-250 nm AlGaIn multiple quantum well light emitting diodes. *Appl. Phys. Lett.* **105**, 051113 (2014)
32. H. Hirayama, N. Maeda, S. Fujikawa, S. Toyoda, N. Kamata, Recent progress and future prospects of AlGaIn-based high-efficiency deep-ultraviolet light-emitting diodes. *Jpn. J. Appl. Phys.* **53**, 100209 (2014)
33. Information on low and medium pressure mercury lamps. Retrieved 5 Oct 2015, [www.heraeus-noblelight.com](http://www.heraeus-noblelight.com)
34. W.L. Morison, *Phototherapy and Photochemotherapy of Skin Disease*, 2nd edn. (Raven Press, New York, 1991)
35. P.E. Hockberger, A history of ultraviolet photobiology for humans, animals and microorganisms. *Photochem. Photobiol.* **76**(6), 561–579 (2002)
36. M. Schreiner, J. Martínez-Abaigar, J. Glaab, M. Jansen, UVB induced secondary plant metabolites. *Optik Photonik* **9**(2), 34–37 (2014)
37. S. Vilhunen, H. Särkkä, M. Sillanpää, Ultraviolet light-emitting diodes in water disinfection. *Environ. Sci. Pollut. Res.* **16**(4), 439–442 (2009)
38. M.H. Crawford, M.A. Banas, M.P. Ross, D.S. Ruby, J.S. Nelson, R. Boucher, A.A. Allerman, Final LDRD report: ultraviolet water purification systems for rural environments and mobile applications. Sandia Report, SAND2005-7245 (2005)

39. M.A. Würtele, T. Kolbe, M. Lipsz, A. Külberg, M. Weyers, M. Kneissl, M. Jekel, Application of GaN-based deep ultraviolet light emitting diodes—UV-LEDs—for Water disinfection. *Water Res.* **45**(3), 1481 (2011)
40. W. Kowalski, *Ultraviolet Germicidal Irradiation Handbook* (Springer-Verlag, Berlin, Heidelberg, 2009)
41. G.Y. Lui, D. Roser, R. Corkish, N. Ashbolt, P. Jagals, R. Stuetz, Photovoltaic powered ultraviolet and visible light-emitting diodes for sustainable point-of-use disinfection of drinking waters. *Sci. Total Environ.* **493**, 185 (2014)
42. J. Mellqvist, A. Rosen, DOAS for flue gas monitoring—temperature effects in the UV/visible absorption spectra of NO, NO<sub>2</sub>, SO<sub>2</sub>, and NH<sub>3</sub>. *J. Quant. Spectrosc. Radiat. Transf.* **56**(2), 187–208 (1996)
43. J. Hodgkinson, R.P. Tatam, Optical gas sensing: a review. *Meas. Sci. Technol.* **24**, 012004 (2013)
44. P.J. Hargis Jr, T.J. Sobering, G.C. Tisone, J.S. Wagner, Ultraviolet fluorescence detection and identification of protein, DNA, and bacteria. *Proc. SPIE* **2366**, 147 (1995)
45. Z. Xu, B.M. Sadler, Ultraviolet communications: potential and state-of-the-art. *IEEE Commun. Mag.* **67** (2008)
46. K.-X. Sun, B. Allard, S. Buchman, S. Williams, R.L. Byer, LED deep UV source for charge management of gravitational reference sensors. *Class. Quantum Grav.* **23**, S141–S150 (2006)
47. “UV-LED market to grow from \$90 m to \$520 m in 2019”. Retrieved 5 Oct 2015, [www.semiconductor-today.com](http://www.semiconductor-today.com) *Semicond. Today* **10**(1), 80 (2015)
48. F. Mehnke, Institute of Solid State Physics, TU Berlin, private communication (2014)
49. T. Whitaker, Rubicon technology demonstrates 12-inch sapphire wafers. [www.ledsmagazine.com/articles/2011/01/rubicon-technology-demonstrates-12-inch-sapphire-wafers.html](http://www.ledsmagazine.com/articles/2011/01/rubicon-technology-demonstrates-12-inch-sapphire-wafers.html)
50. F. Brunner, H. Protzmann, M. Heuken, A. Knauer, M. Weyers, M. Kneissl, High-temperature growth of AlN in a Production Scale 11x2” MOVPE reactor. *Phys. Stat. Sol. (c)* **1** (2008)
51. O. Reentilä, F. Brunner, A. Knauer, A. Mogi-latenko, W. Neumann, H. Protzmann, M. Heuken, M. Kneissl, M. Weyers, G. Tränkle, Effect of the AlN nucleation layer growth on AlN material qual-ity. *J. Cryst. Growth* **310**(23), 4932 (2008)
52. V. Kueller, A. Knauer, F. Brunner, A. Mogilatenko, M. Kneissl, M. Weyers, Investigation of inversion domain formation in AlN grown on sapphire by MOVPE. *Phys. Stat. Sol. (c)* **9**(3–4), 496–498 (2012)
53. D.A.B. Miller, D.S. Chemla, T.C. Damen, A.C. Gossard, W. Wiegmann, T.H. Wood, C.A. Burrus, Band-edge electroabsorption in quantum Weil structures: the quantum-confined stark effect. *Phys. Rev. Lett.* **53**(22), 2173 (1984)
54. J. Simon, V. Protasenko, C. Lian, H. Xing, D. Jena, Polarization-induced hole doping in wide-band-gap uniaxial semiconductor heterostructures. *Science* **327**, 60 (2009)
55. Y. Liao, C. Thomidis, C. Kao, T.D. Moustakas, AlGaIn based deep ultraviolet light emitting diodes with high internal quantum efficiency grown by molecular beam epitaxy. *Appl. Phys. Lett.* **98**, 081110 (2011)
56. S. Kurin, A. Antipov, I. Barash, A. Roenkov, A. Usikov, H. Helava, V. Ratnikov, N. Shmidt, A. Sakharov, S. Tarasov, E. Menkovich, I. Lamkin, B. Papchenko, Y. Makarov, Characterization of HVPE-grown UV LED heterostructures. *Phys. Stat. Sol. (c)* **11**(3–4), 813 (2014)
57. S.F. Chichibu, A. Uedono, T. Onuma, B.A. Haskell, A. Chakraborty, T. Koyama, P.T. Fini, S. Keller, S.P. DenBaars, J.S. Speck, U.K. Mishra, S. Nakamura, S. Yamaguchi, S. Kamiyama, H. Amano, I. Akasaki, J. Han, T. Sota, Origin of defect-insensitive emission probability in In-containing (Al, In, Ga)N alloy semiconductors. *Nat. Mater.* **5**, 810–816 (2006)
58. T. Wunderer, C.L. Chua, Z. Yang, J.E. Northrup, N.M. Johnson, G.A. Garrett1, H. Shen1, M. Wraback, Pseudomorphically grown ultraviolet C photopumped lasers on bulk AlN substrates. *Appl. Phys. Express* **4**, 092101 (2011)

59. T. Wunderer, C.L. Chua, J.E. Northrup, Z. Yang, N.M. Johnson, M. Kneissl, G.A. Garrett, H. Shen, M. Wraback, B. Moody, H.S. Craft, R. Schlessler, R.F. Dalmau, Z. Sitar, Optically pumped UV lasers grown on bulk AlN substrates. *Phys. Stat. Sol. (c)* **9**, 822 (2012)
60. Y.C. Shen, G.O. Mueller, S. Watanabe, N.F. Gardner, A. Munkholm, M.R. Krames, Auger recombination in InGaN measured by photoluminescence. *Appl. Phys. Lett.* **91**, 141101 (2007)
61. M.-H. Kim, M.F. Schubert, Q. Dai, J.K. Kim, E. Fred Schubert, J. Piprek, Y. Park, Origin of efficiency droop in GaN-based light-emitting diodes. *Appl. Phys. Lett.* **91**, 183507 (2007)
62. J. Hader, J.V. Moloney, B. Pasenow, S.W. Koch, M. Sabathil, N. Linder, S. Lutgen, On the importance of radiative and Auger losses in GaN-based quantum wells. *Appl. Phys. Lett.* **92**, 261103 (2008)
63. A. Laubsch, M. Sabathil, W. Bergbauer, M. Strassburg, H. Lugauer, M. Peter, S. Lutgen, N. Linder, K. Streubel, J. Hader, J.V. Moloney, B. Pasenow, S.W. Koch, On the origin of IQE-‘droop’ in InGaN LEDs. *Phys. Stat. Sol. (c)* **6**(S2), S913 (2009)
64. J. Cho, E. Fred Schubert, J.K. Kim, Efficiency droop in light-emitting diodes: Challenges and countermeasures. *Laser Photonics Rev.* **7**(3), 408–421 (2013)
65. J. Iveland, L. Martinelli, J. Peretti, J.S. Speck, C. Weisbuch, Direct measurement of auger electrons emitted from a semiconductor light-emitting diode under electrical injection: identification of the dominant mechanism for efficiency droop. *Phys. Rev. Lett.* **110**, 177406 (2013)
66. J. Yun, J.-I. Shim, H. Hirayama, Analysis of efficiency droop in 280-nm AlGaIn multiple-quantum-well light-emitting diodes based on carrier rate equation. *Appl. Phys. Express* **8**, 022104 (2015)
67. E. Kioupakis, P. Rinke, K.T. Delaney, C.G. Van de Walle, Indirect Auger recombination as a cause of efficiency droop in nitride light-emitting diodes. *Appl. Phys. Lett.* **98**, 161107 (2011)
68. K. Ban, J. Yamamoto, K. Takeda, K. Ide, M. Iwaya, T. Takeuchi, S. Kamiyama, I. Akasaki, H. Amano, Internal quantum efficiency of whole-composition-range AlGaIn multiquantum wells. *Appl. Phys. Express* **4**, 052101 (2011)
69. Y. Narukawa, M. Ichikawa, D. Sanga, M. Sano, T. Mukai, White light emitting diodes with super-high luminous efficacy. *J. Phys. D Appl. Phys.* **43**, 354002 (2010)
70. Solid-state lighting research and development: multi-year program plan. U.S. Department of Energy, DOE/EE-1089 (2014)
71. S. Karpov, Y.N. Makarov, Dislocation effect on light emission in gallium nitride. *Appl. Phys. Lett.* **81**, 4721 (2002)
72. C. Reich, M. Feneberg, V. Kueller, A. Knauer, T. Wernicke, J. Schlegel, M. Frentrup, R. Goldhahn, M. Weyers, M. Kneissl, Excitonic recombination in epitaxial lateral overgrown AlN on sapphire. *Appl. Phys. Lett.* **103**, 212108 (2013)
73. V. Kueller, A. Knauer, F. Brunner, U. Zeimer, H. Rodriguez, M. Weyers, M. Kneissl, Growth of AlGaIn and AlN on patterned AlN/sapphire templates. *J. Cryst. Growth* **315**(1), 200 (2011)
74. V. Kueller, A. Knauer, U. Zeimer, M. Kneissl, M. Weyers, Controlled coalescence of MOVPE grown AlN during lateral overgrowth. *J. Cryst. Growth* **368**, 83 (2013)
75. U. Zeimer, V. Kueller, A. Knauer, A. Mogilatenko, M. Weyers, M. Kneissl, High quality AlGaIn grown on ELO AlN/sapphire templates. *J. Cryst. Growth* **377**, 32 (2013)
76. M. Martens, F. Mehne, C. Kuhn, C. Reich, T. Wernicke, J. Rass, V. Küller, A. Knauer, C. Netzel, M. Weyers, M. Bickermann, M. Kneissl, Performance characteristics of UVC AlGaIn-based lasers grown on sapphire and bulk AlN substrates. *IEEE Photonics Tech. Lett.* **26**, 342 (2014)
77. M. Kim, T. Fujita, S. Fukahori, T. Inazu, C. Pernot, Y. Nagasawa, A. Hirano, M. Ippommatsu, M. Iwaya, T. Takeuchi, S. Kamiyama, M. Yamaguchi, Y. Honda, H. Amano, I. Akasaki, AlGaIn-based deep ultraviolet light-emitting diodes fabricated on patterned sapphire substrates. *Appl. Phys. Express* **4**, 092102 (2011)

78. J. Rass, T. Kolbe, N. Lobo Ploch, T. Wernicke, F. Mehnke, C. Kuhn, J. Enslin, M. Guttman, C. Reich, J. Glaab, C. Stoelmacker, M. Lapeyrade, S. Einfeldt, M. Weyers, M. Kneissl, High power UV-B LEDs with long lifetime. *Proc. SPIE* **9363**, 93631K (2015)
79. K. Forghani, M. Klein, F. Lipski, S. Schwaiger, J. Hertkorn, R.A.R. Leute, F. Scholz, M. Feneberg, B. Neuschl, K. Thonke, O. Klein, U. Kaiser, R. Gutt, T. Passow, High quality AlGaIn epilayers grown on sapphire using SiN<sub>x</sub> interlayers. *J. Cryst. Growth* **315**, 216–219 (2011)
80. C.G. Van de Walle, J. Neugebauer, First-principles calculations for defects and impurities: applications to III-nitrides. *J. Appl. Phys.* **95**(8), 3851 (2004)
81. M.A. Reshchikova, H. Morkoç, Luminescence properties of defects in GaN. *J. Appl. Phys.* **97**, 061301 (2005)
82. S.F. Chichibu, T. Onuma, K. Hazu, A. Uedono, Major impacts of point defects and impurities on the carrier recombination dynamics in AlN. *Appl. Phys. Lett.* **97**, 201904 (2010)
83. T.A. Henry, A. Armstrong, A.A. Allerman, M.H. Crawford, The influence of Al composition on point defect incorporation in AlGaIn. *Appl. Phys. Lett.* **100**, 043509 (2012)
84. J. Carlos Rojo, G.A. Slack, K. Morgan, B. Raghathamachar, M. Dudley, L.J. Schowalter, Report on the growth of bulk aluminum nitride and subsequent substrate preparation. *J. Cryst. Growth* **231**, 317 (2001)
85. Z.G. Herro, D. Zhuang, R. Schlessner, Z. Sitar, Growth of AlN single crystalline boules. *J. Cryst. Growth* **312**, 2519–2521 (2010)
86. M. Bickermann, B.M. Epelbaum, O. Filip, P. Heimann, S. Nagata, A. Winnacker, UV transparent single-crystalline bulk AlN substrates. *Phys. Stat. Sol. (C)* **7**(1), 21 (2010)
87. C. Hartmann, J. Wollweber, A. Dittmar, K. Irmscher, A. Kwasniewski, F. Langhans, T. Neugut, M. Bickermann, Preparation of bulk AlN seeds by spontaneous nucleation of freestanding crystals. *Jpn. J. Appl. Phys.* **52**, 08JA06 (2013)
88. R. Collazo, J. Xie, B.E. Gaddy, Z. Bryan, R. Kirste, M. Hoffmann, R. Dalmau, B. Moody, Y. Kumagai, T. Nagashima, Y. Kubota, T. Kinoshita, A. Koukitu, D.L. Irvine, Z. Sitar, On the origin of the 265 nm absorption band in AlN bulk crystals. *Appl. Phys. Lett.* **100**, 191914 (2012)
89. K. Irmscher, C. Hartmann, C. Gugushev, M. Pietsch, J. Wollweber, M. Bickermann, Identification of a tri-carbon defect and its relation to the ultraviolet absorption in aluminum nitride. *J. Appl. Phys.* **114**, 123505 (2013)
90. B.E. Gaddy, Z. Bryan, I. Bryan, J. Xie, R. Dalmau, B. Moody, Y. Kumagai, T. Nagashima, Y. Kubota, T. Kinoshita, A. Koukitu, R. Kirste, Z. Sitar, R. Collazo, D.L. Irving, The role of the carbon-silicon complex in eliminating deep ultraviolet absorption in AlN. *Appl. Phys. Lett.* **104**, 202106 (2014)
91. Y. Kumagai, Y. Kubota, T. Nagashima, T. Kinoshita, R. Dalmau, R. Schlessner, B. Moody, J. Xie, H. Murakami, A. Koukitu, Z. Sitar, Preparation of a freestanding AlN substrate from a thick AlN layer grown by hydride vapor phase epitaxy on a bulk AlN substrate prepared by physical vapor transport. *Appl. Phys. Express* **5**, 055504 (2012)
92. T. Kinoshita, K. Hironaka, T. Obata, T. Nagashima, R. Dalmau, R. Schlessner, B. Moody, J. Xie, S. Inoue, Y. Kumagai, A. Koukitu, Z. Sitar, Deep-ultraviolet light-emitting diodes fabricated on AlN substrates prepared by hydride vapor phase epitaxy. *Appl. Phys. Express* **5**, 122101 (2012)
93. K.B. Nam, M.L. Nakarmi, J. Li, J.Y. Lin, H.X. Jiang, Mg acceptor level in AlN probed by deep ultraviolet photoluminescence. *Appl. Phys. Lett.* **83**(5), 878 (2003)
94. M.L. Nakarmi, K.H. Kim, M. Khizar, Z.Y. Fan, J.Y. Lin, H.X. Jiang, Electrical and optical properties of Mg-doped Al<sub>0.7</sub>Ga<sub>0.3</sub>N alloys. *Appl. Phys. Lett.* **86**, 092108 (2005)
95. X.T. Trinh, D. Nilsson, I.G. Ivanov, E. Janzén, A. Kakanakova-Georgieva, N.T. Son, Stable and metastable Si negative-U centers in AlGaIn and AlN. *Appl. Phys. Lett.* **105**, 162106 (2014)



96. A. Kakanakova-Georgieva, D. Nilsson, X.T. Trinh, U. Forsberg, N.T. Son, E. Janzen, The complex impact of silicon and oxygen on the n-type conductivity of high-Al-content AlGa<sub>N</sub>. *Appl. Phys. Lett.* **102**, 132113 (2013)
97. J.R. Grandusky, J.A. Smart, M.C. Mendrick, L.J. Schowalter, K.X. Chen, E.F. Schubert, Pseudomorphic growth of thick n-type Al<sub>x</sub>Ga<sub>1-x</sub>N layers on low-defect-density bulk AlN substrates for UV LED applications. *J. Cryst. Growth* **311**, 2864 (2009)
98. B. Cheng, S. Choi, J.E. Northrup, Z. Yang, C. Knollenberg, M. Teepe, T. Wunderer, C.L. Chua, N.M. Johnson, Enhanced vertical and lateral hole transport in high aluminum-containing AlGa<sub>N</sub> for deep ultraviolet light emitters. *Appl. Phys. Lett.* **102**, 231106 (2013)
99. A.A. Allerman, M.H. Crawford, M.A. Miller, S.R. Lee, Growth and characterization of Mg-doped AlGa<sub>N</sub>-AlN short-period superlattices for deep-UV optoelectronic devices. *J. Cryst. Growth* **312**, 756–761 (2010)
100. J. Simon, V. Protasenko, C. Lian, H. Xing, D. Jena, Polarization-induced hole doping in wide-band-gap uniaxial semiconductor heterostructures. *Science* **327**, 60 (2010)
101. R. Dahal, J. Li, S. Majety, B.N. Pantha, X.K. Cao, J.Y. Lin, H.X. Jiang, Epitaxially grown semiconducting hexagonal boron nitride as a deep ultraviolet photonic material. *Appl. Phys. Lett.* **98**, 211110 (2011)
102. R. Collazo, S. Mita, J. Xie, A. Rice, J. Tweedie, R. Dalmau, Z. Sitar, Progress on n-type doping of AlGa<sub>N</sub> alloys on AlN single crystal substrates for UV optoelectronic applications. *Phys. Stat. Sol. (c)* **8**(7–8), 2031 (2011)
103. F. Mehnke, T. Wernicke, H. Pinhel, C. Kuhn, C. Reich, V. Kueller, A. Knauer, M. Lapeyrate, M. Weyers, M. Kneissl, Highly conductive n-Al<sub>x</sub>Ga<sub>1-x</sub>N layers with aluminum mole fractions above 80 %. *Appl. Phys. Lett.* **103**, 212109 (2013)
104. S. Ruvimov, Z. Liliental-Weber, J. Washburn, D. Qiao, S.S. Lau, P.K. Chu, Microstructure of Ti/Al ohmic contacts for n-AlGa<sub>N</sub>. *Appl. Phys. Lett.* **73**, 2582 (1998)
105. J.H. Wang, S.E. Mohney, S.H. Wang, U. Chowdhury, R.D. Dupuis, Vanadium-based ohmic contacts to n-type Al<sub>0.6</sub>Ga<sub>0.4</sub>N. *J. Electron. Mater.* **33**, 418 (2004)
106. R. France, T. Xu, P. Chen, R. Chandrasekaran, T.D. Moustakas, Vanadium-based Ohmic contacts to n-AlGa<sub>N</sub> in the entire alloy composition. *Appl. Phys. Lett.* **90**, 062115 (2007)
107. M. Lapeyrate, A. Muhin, S. Einfeldt, U. Zeimer, A. Mogilatenko, M. Weyers, M. Kneissl, Electrical properties and microstructure of vanadium-based contacts on ICP plasma etched n-type AlGa<sub>N</sub>:Si and GaN:Si surfaces. *Semicond. Sci. Technol.* **28**, 125015 (2013)
108. M. Lapeyrate, F. Eberspach, N. Lobo Ploch, C. Reich, M. Guttman, T. Wernicke, F. Mehnke, S. Einfeldt, A. Knauer, M. Weyers, M. Kneissl, Current spreading study in UVC LED emitting around 235 nm. *Proc. SPIE* **9363**, 93631P (2015)
109. I.E. Titkov, D.A. Sannikov, Y.-M. Park, J.K. Son, Blue light emitting diode internal and injection efficiency. *AIP Adv.* **2**, 032117 (2012)
110. N. Lobo-Ploch, Chip designs for high efficiency III-nitride based ultraviolet light emitting diodes with enhanced light extraction. Ph.D. Thesis (2015)
111. A. Khan, K. Balakrishnan, T. Katona, Ultraviolet light-emitting diodes based on group three nitrides. *Nat. Photonics* **2**, 77 (2008)
112. V. Adivarahan, A. Heidari, B. Zhang, Q. Fareed, S. Hwang, M. Islam, A. Khan, 280 nm deep ultraviolet light emitting diode lamp with an AlGa<sub>N</sub> multiple quantum well active region. *Appl. Phys. Express* **2**, 102101 (2009)
113. L. Zhou, J.E. Epler, M.R. Krames, W. Goetz, M. Gherasimova, Z. Ren, J. Han, M. Kneissl, N.M. Johnson, Vertical injection thin-film AlGa<sub>N</sub>/AlGa<sub>N</sub> multiple-quantum-well deep ultraviolet light-emitting diodes. *Appl. Phys. Lett.* **89**, 241113 (2006)
114. T.N. Oder, K.H. Kim, J.Y. Lin, H.X. Jiang, III-nitride blue and ultraviolet photonic crystal light emitting diodes. *Appl. Phys. Lett.* **84**, 466 (2004)
115. T. Gessmann, E.F. Schubert, J.W. Graff, K. Streubel, C. Karnutsch, Omnidirectional reflective contacts for light-emitting diodes. *IEEE Electron Device Lett.* **24**(10), 683 (2003)

116. N. Lobo, H. Rodriguez, A. Knauer, M. Hoppe, S. Einfeldt, P. Vogt, M. Weyers, M. Kneissl, Enhancement of light extraction in UV LEDs using nanopixel contact design with Al reflector. *Appl. Phys. Lett.* **96**, 081109 (2010)
117. K.B. Nam, J. Li, M.L. Nakarmi, J.Y. Lin, H.X. Jianga, Unique optical properties of AlGaIn alloys and related ultraviolet emitters. *Appl. Phys. Lett.* **84**, 5264 (2004)
118. J.E. Northrup, C.L. Chua, Z. Yang, T. Wunderer, M. Kneissl, N.M. Johnson, T. Kolbe, Effect of strain and barrier composition on the polarization of light emission from AlGaIn/AlN quantum wells. *Appl. Phys. Lett.* **100**, 021101 (2012)
119. T. Kolbe, A. Knauer, C. Chua, Z. Yang, V. Kueller, S. Einfeldt, P. Vogt, N.M. Johnson, M. Weyers, M. Kneissl, Effect of temperature and strain on the optical polarization of (In)(Al) GaN ultraviolet light emitting diodes. *Appl. Phys. Lett.* **99**, 261105 (2011)
120. T. Kolbe, A. Knauer, J. Stellmach, C. Chua, Z. Yang, H. Rodrigues, S. Einfeldt, P. Vogt, N. M. Johnson, M. Weyers, M. Kneissl, Optical polarization of UV-A and UV-B (In)(Al)GaN multiple quantum well light emitting diodes. *Proc. SPIE* **7939**, 79391G (2011)
121. T. Kolbe, A. Knauer, C. Chua, Z. Yang, H. Rodrigues, S. Einfeldt, P. Vogt, N.M. Johnson, M. Weyers, M. Kneissl, Optical polarization characteristics of ultraviolet (In)(Al)GaN multiple quantum well light emitting diodes. *Appl. Phys. Lett.* **97**, 171105 (2010)
122. J.J. Wierer, I. Montano, M.H. Crawford, A.A. Allerman, Effect of thickness and carrier density on the optical polarization of  $\text{Al}_{0.44}\text{Ga}_{0.56}\text{N}/\text{Al}_{0.55}\text{Ga}_{0.45}\text{N}$  quantum well layers. *J. Appl. Phys.* **115**, 174501 (2014)
123. J.J. Wierer Jr, A.A. Allerman, I. Montano, M.W. Moseley, Influence of optical polarization on the improvement of light extraction efficiency from reflective scattering structures in AlGaIn ultraviolet light-emitting diodes. *Appl. Phys. Lett.* **105**, 061106 (2014)
124. H.-Y. Ryu, I.-G. Choi, H.-S. Choi, J.-I. Shim, Investigation of light extraction efficiency in AlGaIn deep-ultraviolet light-emitting diodes. *Appl. Phys. Express* **6**, 062101 (2013)
125. N. Lobo Ploch, H. Rodriguez, C. Stölmacker, M. Hoppe, M. Lapeyrade, J. Stellmach, F. Mehnke, T. Wernicke, A. Knauer, V. Kueller, M. Weyers, S. Einfeldt, M. Kneissl, Effective thermal management in ultraviolet light emitting diodes with micro-LED arrays. *IEEE Trans. Electron Devices* **60**(2), 782–786 (2013)
126. N. Lobo Ploch, S. Einfeldt, T. Kolbe, A. Knauer, M. Frentrop, V. Kueller, M. Weyers, M. Kneissl, Investigation of the temperature dependent efficiency droop in UV LEDs. *Semicond. Sci. Technol.* **28**, 125021 (2013)
127. M. Shatalov, W. Sun, R. Jain, A. Lunev, X. Hu, A. Dobrinsky, Y. Bilenko, J. Yang, G.A. Garrett, L.E. Rodak, M. Wraback, M. Shur, R. Gaska, High power AlGaIn ultraviolet light emitters. *Semicond. Sci. Technol.* **29**, 084007 (2014)
128. P. Scheidt, Thermal management of LED technology in applications. *LED Prof. Rev.* **19** (2007), Retrieved 7 Oct 2014, [www.led-professional.com](http://www.led-professional.com).
129. R. Huber, Thermal management in high power LED systems. *LED Prof. Rev.* **22** (2007), Retrieved 7 Oct 2014, [www.led-professional.com](http://www.led-professional.com).
130. J. Glaab, C. Ploch, R. Kelz, C. Stölmacker, M. Lapeyrade, N. Lobo Ploch, J. Rass, T. Kolbe, S. Einfeldt, F. Mehnke, C. Kuhn, T. Wernicke, M. Weyers, M. Kneissl, Temperature induced degradation of InAlGaIn multiple-quantum well UV-B LEDs. *MRS Proc.* **1792**, mrrs15-2102646 (2015)
131. J. Glaab, C. Ploch, R. Kelz, C. Stoelmacker, M. Lapeyrade, N. Lobo Ploch, J. Rass, T. Kolbe, S. Einfeldt, F. Mehnke, C. Kuhn, T. Wernicke, M. Weyers, M. Kneissl, Degradation of (InAlGa)N-based UV-B LEDs stressed by current and temperature. *J. Appl. Phys.* **118**(9), 094504 (2015)
132. C.G. Moe, J.R. Grandusky, J. Chen, K. Kitamura, M.C. Mendrick, M. Jamil, M. Toita, S.R. Gibb, L.J. Schowalter, High-power pseudomorphic mid-ultraviolet light-emitting diodes with improved efficiency and lifetime. *Proc. SPIE* **8986**, 89861V (2014)
133. M. Meneghini, M. Pavesi, N. Trivellin, R. Gaska, E. Zanoni, G. Meneghesso, Reliability of deep-UV light-emitting diodes. *IEEE Trans. Device Mater. Reliab.* **8**(2), 248 (2008)

134. M. Meneghini, D. Barbisan, L. Rodighiero, G. Meneghesso, E. Zanoni, Analysis of the physical processes responsible for the degradation of deep-ultraviolet light emitting diodes. *Appl. Phys. Lett.* **97**, 143506 (2010)
135. H. Amano, I. Akasaki, GaN blue and ultraviolet light emitting devices. *Solid State Phys.* **25**, 399 (1990)
136. A. Chitnis, A. Kumar, M. Shatalov, V. Adivarahan, A. Lunev, J.W. Yang, G. Simin, M.A. Khan, R. Gaska, M. Shur, High-quality p-n junctions with quaternary AlInGaN/InGaN quantum wells. *Appl. Phys. Lett.* **77**, 3880–3882 (2000)
137. V. Adivarahan, S. Wu, A. Chitnis, R. Pachipulusu, V. Mandavilli, M. Shatalov, J.P. Zhang, M. Asif Khan, G. Tamulaitis, I. Yilmaz, M.S. Shur, R. Gaska, AlGaIn single-quantum-well light-emitting diodes with emission at 285 nm. *Appl. Phys. Lett.* **81**(19), 3666 (2002)
138. A. Chitnis, J.P. Zhang, V. Adivarahan, W. Shuai, J. Sun, M. Shatalov, J.W. Yang, G. Simin, M. Asif Khan, 324 nm light emitting diodes with milliwatt powers. *Jpn. J. Appl. Phys.* **41** (Part 2), 4B, L450 (2002)

<http://www.springer.com/978-3-319-24098-5>

III-Nitride Ultraviolet Emitters

Technology and Applications

Kneissl, M.; Rass, J. (Eds.)

2016, XIX, 442 p. 241 illus., 158 illus. in color.,

Hardcover

ISBN: 978-3-319-24098-5